Optics Letters

# Reconfigurable semiconductor laser networks based on diffractive coupling

DANIEL BRUNNER* AND INGO FISCHER

[1]Instituto de Física Interdisciplinar y Sistemas Complejos, IFISC (UIB-CSIC), Campus Universitat de les Illes Balear, E-07122 Palma de Mallorca, Spain
*Corresponding author: dbrunner@ifisc.uib-csic.es

Received 12 June 2015; revised 24 July 2015; accepted 24 July 2015; posted 27 July 2015 (Doc. ID 242821); published 11 August 2015

**Networks of optical emitters are highly sought-after, both for fundamental investigations as well as for various technological applications. We introduce and implement a novel scheme, based on diffractive optical coupling, allowing for the coupling of large numbers of optical emitters with adjustable weights. We demonstrate its potential by coupling emitters of a 2D array of semiconductor lasers with significant efficiency.** 

***OCIS codes:*** (250.7260) Vertical cavity surface emitting lasers; (200.4260) Neural networks; (190.3100) Instabilities and chaos.

http://dx.doi.org/10.1364/OL.40.003854

Coupling lasers in a scalable fashion while providing control over individual connections are a highly sought-after technology, impacting upon a large range of scientific questions and engineering challenges. In engineering, arrays of phase-locked lasers would significantly boost the brightness of material-processing systems [1] or enable beam-steering via a phased-array without the need for moving parts [2]. In the field of nonlinear network dynamics, semiconductor laser networks are prominent model systems [3]. In information processing, laser networks are highly attractive for the implementation of either neuro-inspired computing [4,5] or for all-optical Ising machines based on coherent computing [6]. Fundamental properties of semiconductor-laser networks like synchronization, phase-locking, and consistency, are of considerable interest and essential for future applications based on such systems. Nonetheless, until today, no scalable approach for creating such networks exists that simultaneously provides control over essential parameters such as the network's coupling topology. As a consequence, experimental results are lacking.

One of the most commonly attempted techniques for the implementation of global coupling within an array of lasers employs Talbot self-imaging [7]. Until today, however, no successful creation of large, scalable, and reconfigurable laser network has been demonstrated. Furthermore, the Talbot architecture requires locked and in-phase emission of all emitters. This results in a strong limitation of the dynamical regimes resulting in efficient coupling using Talbot architectures. Chaotic dynamics is often associated with nonconstructive interference and nonconstant phase relations. Other techniques utilize gratings to lock the wavelengths of all elements within an array of lasers [8]. Although this technique appears robust and scalable, it does not establish coupling between emitters. Finally, for solid-state lasers, a coupling scheme enabling some control over the network topology has been reported [9]. Here, the number of possible coupling paths is effectively limited, since each connection symmetry requires a dedicated mirror. We utilize the diffractive orders of a diffractive-optical element (DOE), placed within an external cavity, combined with an imaging lens to create coupling within the emitters of a laser array. With our scheme, coupling between a laser and its neighbors is established and can be adjusted in a programmable fashion. Furthermore, in our current setup, we identify imaging aberrations as the limiting factor for both, network size and coupling strength. Consequently, significantly larger networks are possible with our diffractive coupling scheme. Finally, we evaluate and confirm the scalability of our diffractive-coupling method.

Our diffractive-optical network, illustrated in Fig. 1, is based on an 8 × 8 array of single-mode vertical-cavity surface-emitting lasers (VCSELs) from Princeton Optronics, arranged in a square lattice with a pitch of 250 μm. Its optical emission passes the DOE and is imaged by a lens (Thorlabs AL 1225-B, $f = 25$ mm) located at object distance $d_2$ from the VCSEL array. The image created at image distance $d_1$ results in an angular offset ($\phi_i^{\pm}$) between laser $i$ and its nearest neighbors, which is continuously adjustable via $d_2$. Each VCSEL's image is spatially duplicated by the DOE's diffractive orders, resulting in angle $\theta_i^{\pm}$ between the ±1 and 0th diffractive orders for laser $i$. $\phi_i^{\pm}$ and $\theta_i^{\pm}$ are derived directly using the aberration free lens and the grating equation, respectively:

$$\Delta\phi_i^{\pm} = \arctan\left(\frac{r_i}{d_2} \pm \frac{p}{d_2}\right) - \phi_i, \tag{1a}$$

$$\Delta\theta_i^{\pm} = \arcsin\left(\frac{r_i}{\sqrt{r_i^2 + d_2^2}} \pm \frac{a}{\lambda}\right) - \phi_i, \tag{1b}$$

where $a$ is the gratings period and $\lambda$ is the array's wavelength, $r_i$ the laser's distance from the array's center, and $d_2$ is the object distance. Using approximations $\arctan(x) \approx \arcsin(x) \approx x$ and

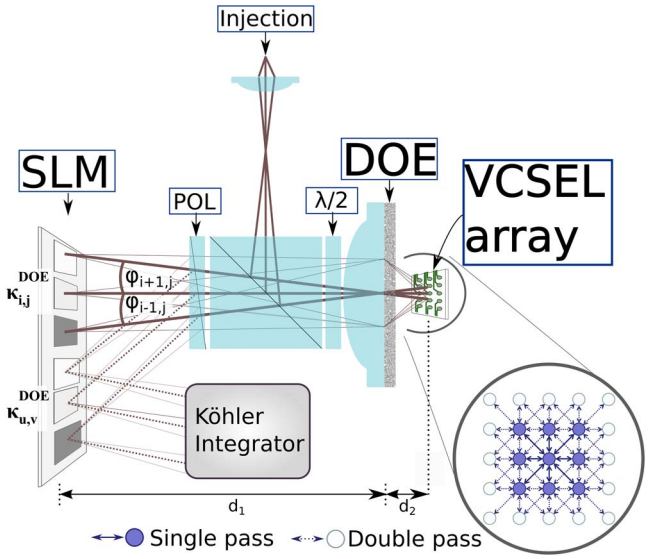


**Fig. 1.** Schematic of the diffractive coupling of an optical array. The VCSEL array's emission passes a diffractive optical element and is imaged onto a reflective spatial-light modulator. The DOE's diffractive side orders overlap with the zero diffractive order of their neighboring lasers for correct adjustment of $\frac{d_1}{d_2}$. The reflection of the spatial light modulator is then again imaged onto the laser array, where the overlapping orders result in coupling between neighboring emitters.

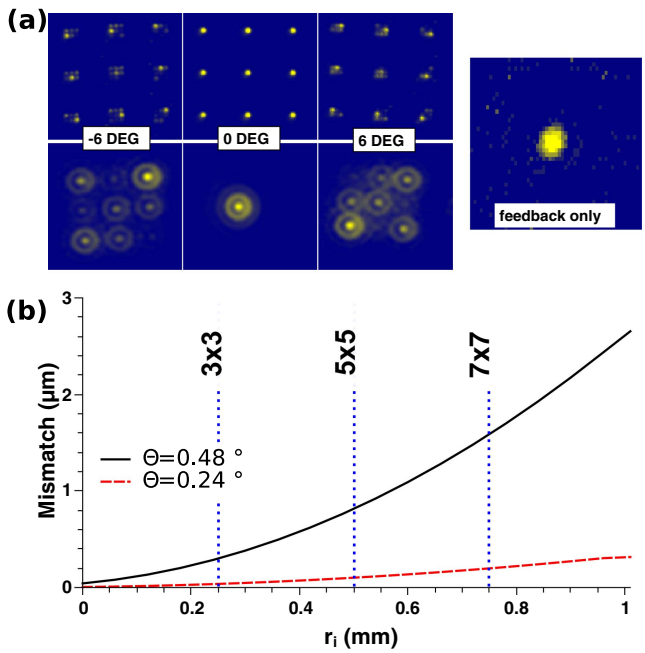


**Fig. 2.** Diffractive coupling images are depicted in panel (a). At 0 deg rotation between array and DOE, the images of neighboring laser emissions overlap. (b) shows the mismatch between imaging and diffractive coupling.

$r_i/\sqrt{r_i^2+d_2^2} \approx r_i/d_2$, valid for small angles $\phi_i$, one can derive an alignment-condition from Eqs. (1a) and (1b):

$$\frac{p}{d_2} = \frac{a}{\lambda} = \sin(\Theta), \tag{2}$$

for which $\Delta\phi_i^{\pm} \approx \Delta\theta_i^{\pm}$. In our experiment, a DOE with diffraction angle $\Theta$ replaces the diffraction grating, and we satisfy Eq. (2) by adjusting $d_2$. Coupling is finally achieved by reflecting the overlapping diffracted laser images back onto the array by situating a reflective surface at distance $d_1$ from the objective lens.

Figure 2 illustrates alignment and scaling properties of the diffractive coupling. Despite the large lattice pitch of 250 μm, due to the large object distance in our setup ($d_2 \approx 30$ mm), the small-angle approximation is justified for the central emitters in our array. In panel (a), we show images of a 3 × 3-array of emitting VCSELs for different DOE rotation angles. The images were created by sampling the array's emission via a beamsplitter (not shown in Fig. 1) using a CCD camera at a distance $d_1$. The upper half in panel (a) shows the Airy discs for all nine diffracted VCSELs for different angles when rotating the DOE around the optical axis. DOE rotation induces rotation of the diffraction side orders around the 0th order for each laser. The lower half of panel (a) magnifies on a single laser's position, demonstrating that for aligned angles, the Airy-discs overlap perfectly, even up to the Airy disc's side-maxima. The image on the right shows the optical feedback from eight surrounding lasers at the position of a deactivated central laser. Again, all of the eight feedback contributions are located perfectly on top of the deactivated central element.

Unfortunately, the small angle approximation restricts $\phi_i$ and $\theta_i$. In our setup, pitch $p$, angle $\Theta$, and as a consequence distance $d_2$ due to Eq. (2) are fixed. Hence the small-angle approximation required for coupling directly limits distance $r_i$. Using Eqs. (1a) and (1b), in Fig. 2(b), we plot the mismatch between the imaging and the diffraction locations at position $d_1$ in dependence on $r_i$. At the array's emission wavelength (966 nm), we obtain $\Theta = 0.48°$. Considering our VCSEL's aperture diameter (∼4 μm FWHM), one can infer from Fig. 2(b) that currently effective coupling is limited to the emitters within the 7 × 7 array. Already for a diffraction angle half as large ($\Theta = 0.24°$), the possible range of $r_i$ would significantly be extended to multiple millimeters. We therefore conclude that our scheme allows for scalable coupling of optical emitters, especially when considering the strong potential for reducing $\Theta$ due to the small pitches $p$ achievable with semiconductor technology.

Optical feedback and therefore coupling are created by placing a spatial light modulator (SLM, Holoeye) at distance $d_1$, enabling control over individual coupling strengths via the programmable spatial reflectivity of the SLM. The feedback-induced laser-to-laser coupling is affected by two attenuation matrices: the DOE's fixed splitting ratio and its efficiency $\boldsymbol{k}^{\mathrm{DOE}}$, and adjustable attenuations controlled by the SLM's gray scale values $\boldsymbol{k}^{\mathrm{SLM}}$. For each laser, $\boldsymbol{k}^{\mathrm{DOE}}$ and $\boldsymbol{k}^{\mathrm{SLM}}$ are 3 × 3 matrices. The optical intensity ($I^{\mathrm{BR}}_{k,l}$) back-reflected of the $(k, l)$th SLM area therefore contains array-scaled contributions from 8 neighbors. Following the back-reflection off the DOE, the optical signal passes the DOE a second time. Hence, the final optical feedback to laser $(p, q)$ is

$$I^{\mathrm{FB}}_{p,q} = \sum_{m,n}^{-1,0,1} \kappa^{\mathrm{DOE}}_{m,n} \cdot \kappa^{\mathrm{SLM}}_{p+m,q+n} \cdot \sum_{i,j}^{-1,0,1} \kappa^{\mathrm{DOE}}_{i,j} \cdot I^{\mathrm{array}}_{p+m+i,q+n+j}. \tag{3}$$

In this equation, $I^{\mathrm{array}}_{i,j}$ and $I^{\mathrm{FB}}_{i,j}$ are the intensities emitted and coupling received by laser $(i, j)$. Expressing Eq. (3) in matrix

form allows to determine $\boldsymbol{k}^{\mathrm{SLM}}$ for a certain coupling matrix $\mathbf{I}^{\mathrm{FB}}$:

$$\mathbf{I}^{\mathrm{FB}} = \boldsymbol{k}^{\mathrm{DOE}} * [\boldsymbol{k}^{\mathrm{SLM}} \cdot (\boldsymbol{k}^{\mathrm{DOE}} * \mathbf{I}^{\mathrm{array}})], \tag{4a}$$

$$\boldsymbol{k}^{\mathrm{SLM}} = [\mathbf{I}^{\mathrm{FB}} \hat{*} \boldsymbol{k}^{\mathrm{DOE}}] \hat{*} [\tilde{\boldsymbol{k}}^{\mathrm{DOE}} \cdot \tilde{\mathbf{I}}^{\mathrm{array}}]. \tag{4b}$$

Symbols $*$ and $\hat{*}$ correspond to convolutions and deconvolutions, respectively. The condition for arriving at Eq. (4b) is that $\boldsymbol{k}_{\mathrm{DOE}}$ is invertible. According to Eq. (4a), the optical feedback is twice convoluted by $\boldsymbol{k}_{\mathrm{DOE}}$. As a consequence, each laser is coupled to a $5 \times 5$ array of its neighboring lasers, enabling a dense connectivity for medium-sized networks. Our diffractive coupling scheme could be modified to a single DOE pass architecture. Then, each laser will be coupled to its neighbors according to $\boldsymbol{k}^{\mathrm{DOE}}$, while $\boldsymbol{k}^{\mathrm{SLM}}$ provides a scaling for each laser. Therefore, $I^{\mathrm{FB}}_{i,j} \neq I^{\mathrm{FB}}_{j,i}$ allows for a network structure according to a directed graph.

For dynamical investigations and for optical information processing like all-optical RC [5,10], it is essential to create a weighted sum of all network states. We achieve this functionality by out-coupling a fraction of the emission using a Rochon prism. The out-coupled emission is imaged onto a separate area of the SLM, where it then can be scaled linearly according to gray-scale values $\omega_{r,s}$. Here, the scaled back-reflection $I^{\mathrm{RO}}_{r,s}$ of SLM-area $(r, s)$ is

$$I^{\mathrm{RO}}_{r,s} = \omega^{\mathrm{SLM}}_{r,s} \cdot \sum_{u,v}^{-1,0,1} I^{\mathrm{array}}_{r+u,s+v} \cdot \kappa^{\mathrm{DOE}}_{u,v}. \tag{5}$$

The readout signal $I^{\mathrm{RO}}$ is homogenized by a Köhler Integrator and focused onto a ~100 μm spot, where it can either be detected or collected by a multi-mode optical fiber.

When biasing individual emitters close to threshold, we obtain a threshold reduction due to self-coupling of ~25% for the central $3 \times 3$ array. This value decreases significantly for the outer elements of a $5 \times 5$ array and vanishes for larger distances. This reduction of self-coupling strength, combined with an imaging resolution below the diffraction limit, demonstrates that aberrations so far limit the size of our diffractive network to the central $3 \times 3$-array.

We demonstrate and evaluate diffractive coupling first by examining modifications to the array's emission power, and second by evaluating coupling-induced network dynamics. For the VCSELs in our network to interact resonantly, we minimize their spectral detuning. This was achieved by biasing the VCSELs according to Table 1 ($T_{\mathrm{array}} = 40°\mathrm{C}$, $\lambda_{\mathrm{array}} = 966.92$ nm). According to Table 1, two lasers were not pumped. One was not connected by the array-manufacturer, the other could not be tuned sufficiently to come into resonance. Under these conditions and deactivating all coupling, we measure a free-running-array emission power of $P_0 = 186$ μW. We begin with the basic coupling mechanism of delayed optical self-feedback or self-coupling. Then the emission power increases $P_{\mathrm{SC}} = 195$ μW, corresponding to $P_{\mathrm{SC}} = 1.048 \cdot P_0$. Evaluating the impact of coupling between lasers, we measure a power of $P_{\mathrm{FC}} = 205$ μW ($P_{\mathrm{FC}} = 1.052 \cdot P_{\mathrm{SC}}$) for the fully coupled network.

**Table 1. Bias Current for Array Emission at 966.92 nm**

| | | |
|---|---|---|
| 2.188 mA | 0 mA | 0.658 mA |
| 1.77 mA | 0 mA | 0.908 mA |
| 2.4 mA | 1.189 mA | 1.411 mA |

**Table 2. Diffractive Laser Network Parameters, Bias Currents as in Table 1**

| | | |
|---|---|---|
| Power w/o coupling | 186 μW | $P_0$ |
| Power self-coupling | 195 μW | $P_{\mathrm{SC}} = 1.048 \cdot P_0$ |
| Power full-coupling | 205 μW | $P_{\mathrm{FC}} = 1.102 \cdot P_0$ |
| Coherent locking | | $P_{\mathrm{CL}} = 1.112 \cdot P_{\mathrm{FC}}$ |
| DC-locking fraction | | $\Delta_{inj} = 78\%$ |

We then inject a spectrally aligned external laser into the 7 lasers simultaneously profiting from the DOE's diffraction. For parallel array and injection laser polarization ($s$-polarization), we measure a power increase of $P_{\mathrm{CL}} = 1.112 \cdot P_{\mathrm{FC}}$ due to partial coherent locking of the array to the external injection laser. Biasing according to Table 1 results in a single linear polarization for the array's emission, which we align such that the emission is coupled out of the resonator by the Rochon prism ($p$-polarization state). In this configuration and for strong interaction, the injection laser will lock the array's emission to its own polarization state. We define the injection induced switching contrast $\Delta_{inj}$ as

$$\Delta_{inj} = \frac{I^{p}_{inj} - I^{\mathrm{CT}}_{inj}}{I^{p}_{0}}, \tag{6}$$

where $I^{p}_{inj}$, $I^{p}_{0}$, and $I^{\mathrm{CT}}_{inj}$ are the array's $p$-polarized emission intensity with and without injection, as well as the $s$-polarized injection laser's cross-talk, respectively. Measuring $I^{p}_{inj} = (98.3 \pm 3)$ μW, $I^{p}_{0} = (294 \pm 3)$ μW and $I^{\mathrm{CT}}_{inj} = (34 \pm 1)$ μW, we obtain an injection-laser-induced polarization switching contrast of the VCSEL network of $\Delta_{inj}$ 78% for an injection laser intensity of ~150 μW per array laser.

A general trend for the coupling-induced power modifications emerges from the preceding results. Under the bias condition of Table 1, each investigated coupling configuration resulted in significantly less relative coupling-induced power increase than the ~25% obtained close to solitary laser threshold ($I_{\mathrm{th}} \approx 0.2$ mA). This reduced relative impact is a direct consequence of the laser network's dynamical state. All lasers are coupled and were biased significantly above solitary threshold, therefore very likely rendering them chaotic [11]. Such dynamics strongly limits the power increase, but represents the basis for many fundamental studies and possible applications [12,13]. The impact of our networks impact upon the DC-emission power is summarized in Table 2.

In the following, we focus in more detail on these coupling-induced complex network dynamics. The rf spectrum of the network's intensity dynamics are shown in Fig. 3(a). RF spectra obtained for strong and attenuated coupling are shown in green and black, respectively. The strong (attenuated) coupling corresponds to a gray-scale value of 255 (0) of the SLM, with a coupling attenuation of ≈30% for a gray scale of zero. Apart from the evident modification to the network's dynamics, one can clearly identify peaks corresponding to half the resonator's roundtrip frequency ($2\tau^{-1}$). For polarization maintaining optical coupling, such dynamics are representative for mutually coupled lasers [14], validating the effectiveness of our coupling scheme.

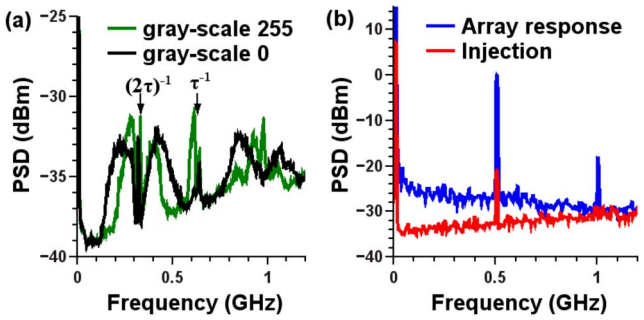


**Fig. 3.** Power spectral density (PSD) for radio-frequency spectra for a free-running network [panel (a)] and the network locked to a modulated external injection laser [panel (b)].

Using insight gained from the rf spectra of Fig. 3(a), we indicate the dynamics present in the network. The dynamics is mainly dominated by the external-cavity roundtrip frequency ($\tau^{-1} \approx 0.65$ GHz) and its higher harmonics, in addition to the coupling-induced component around $(2\tau)^{-1}$. Around those peaks, we find spectrally narrow as well as broad features, indicating a combination of rather periodic and chaotic dynamics. From Table 1, it is clear that for minimized spectral mismatch, the resulting bias currents are widely spread, ranging from $3.3I_{\text{th}} \leq I_{\text{bias}} \leq 12I_{\text{th}}$. This large bias current spread results in equally heterogeneous laser operating conditions, suggesting complex and diverse dynamics. Crucially, the strong modification to the rf spectra induced by the change in coupling strength of the network demonstrates that we are able to sufficiently alter and control the interactions between the lasers. An immediate consequence of the complex network state is that the power increase due to coherent beam combining is limited [12].

Finally, we evaluate the dynamics of our semiconductor laser network under dynamic external injection. For that, the injection laser is modulated with $\nu_{inj} = 0.5$ GHz via a Mach–Zehnder modulator. Detection was limited to the *p*-polarization $I^{p}_{inj}$, and the cross-talk of the *s*-polarized injection laser is shown as red data in Fig. 3(b). Upon injection, the broad rf-spectra consequence of the unlocked network's instabilities [Fig. 3(a)] are quenched by the injection laser. Dynamics of the locked network, shown in Fig. 3(b) as blue data, are therefore dominated by $\nu_{inj}$ (~25 dB suppression). Nonlinear mixing in our laser network causes the additional, spectrally equally sharp frequency component at 1 GHz.

To conclude, we demonstrated a novel diffractive network scheme providing a high level of control over individual network parameters, a global locking to an external injection laser, and the readout of the network's weighted center of mass. We demonstrated strong interaction for the VCSEL array's central elements, showing a significant threshold reduction for an array of 24 lasers. We show that the coupling induces diverse and complex network dynamics, which we are able to modify either via the coupling strength or via an external injection laser. We therefore demonstrate a possibly scalable approach for creating complex networks of optical emitters. This generality makes our diffractive network scheme relevant for a large variety of fields, ranging from fundamental properties of networks of nonlinear elements to more applied fields like reservoir computing, phased arrays, and eventually coherent beam combining. Currently, outside of an area of 500 μm × 500 μm (3 × 3-array), spherical aberrations reduce coupling efficiencies. However, this does not correspond to a fundamental limit since these aberrations can strongly be reduced by use of tailored lenses, a smaller pitch between the lasers, or by a modified resonator design.

For an array of seven spectrally aligned VCSELS, we achieve an emission power increase of 4.2% and 5.1% due to self- and neighbor coupling, respectively. Locking to an external injection laser results in a polarization modulation contrast approaching 80% and an emission power increase by 11.2%, demonstrating partial coherent locking of the array to the injection laser.

**Funding.** Comunitat Autònoma de les Illes Balears (Grups Competitius, FEDER, and MINECO) (TEC2012-36335); European Commission (275840).

## REFERENCES

1. J. R. Leger, G. J. Swanson, and W. B. Veldkamp, Appl. Opt. **26**, 4391 (1987).
2. J. Sun, E. Timurdogan, A. Yaacobi, E. S. Hosseini, and M. R. Watts, Nature **493**, 195 (2013).
3. M. C. Soriano, J. Garcia-Ojalvo, C. R. Mirasso, and I. Fischer, Rev. Mod. Phys. **85**, 421 (2013).
4. F. C. Hoppenstaedt and E. M. Izhikevich, Phys. Rev. E **62**, 4010 (2000).
5. K. Vandoorne, P. Mechet, T. Van Vaerenbergh, M. Fiers, G. Morthier, D. Verstraeten, B. Schrauwen, J. Dambre, and P. Bienstman, Nat. Commun. **5**, 3541 (2014).
6. K. Takata, S. Utsunomiya, and Y. Yamamoto, New J. Phys. **14**, 013052 (2012).
7. V. V. Antyukhov, A. F. Glova, O. R. Kachurin, F. V. Lebedev, V. V. Likhanskii, A. P. Napartovich, and V. D. Pismennyi, JETP Lett. **44**, 78 (1986).
8. N. Trela, H. Baker, and D. Hall, Opt. Express **21**, 4512 (2013).
9. M. Nixon, M. Fridman, E. Ronen, A. A. Friesem, N. Davidson, and I. Kanter, Phys. Rev. Lett. **108**, 214101 (2012).
10. D. Brunner, M. C. Soriano, C. R. Mirasso, and I. Fischer, Nat. Commun. **4**, 1364 (2013).
11. T. Heil, I. Fischer, and W. Elsäßer, J. Opt. B **2**, 413 (2000).
12. B. Liu, Y. Braiman, N. Nair, Y. Lu, Y. Guo, P. Colet, and M. Wardlaw, Opt. Commun. **324**, 301 (2014).
13. S. Heiligenthal, T. Jüngling, O. D'Huys, D. A. Arroyo-Almanza, M. C. Soriano, I. Fischer, I. Kanter, and W. Kinzel, Phys. Rev. E **88**, 012902 (2013).
14. T. Heil, I. Fischer, W. Elsäßer, J. Mulet, and C. R. Mirasso, Phys. Rev. Lett. **86**, 795 (2001).